Solution Phase Behavior and Solid Phase Structure of Long-Chain Sodium Soap Mixtures

Marc N. G. de Mul,*,†,‡ H. Ted Davis,† D. Fennell Evans,† Aparna V. Bhave,§ and James R. Wagner§

Department of Chemical Engineering and Materials Science, University of Minnesota, 421 Washington Avenue SE, Minneapolis, Minnesota 55455, and Imation Corporation, 3M Center Bldg 235-1F-07, St. Paul, Minnesota 55144-1000

Received March 28, 2000. In Final Form: July 11, 2000

Long-chain soaps are generally applied in industrial products as mixtures. For example, photothermographic materials often use a mixture of silver soaps consisting of silver stearate, arachidate, and behenate. Little phase information is available on long-chain soaps and none on soap mixtures, although the phase behavior and microstructure often have a direct effect on product properties. In the present study the Krafft solubility boundaries of sodium stearate, arachidate, and behenate in water were measured for low soap weight fractions. Data for the cmc showed that the observed Krafft boundary lies above the cmc in its entirety for each of the soaps. Therefore, the knee in the Krafft boundary cannot be identified with the formation of micelles. The Krafft temperature of mixtures of these three soaps was observed to have a minimum value at a high content of the shortest-chain soap. The nonlinear relationship between the soap solubility and the mixture composition can be fitted to a mixing rule based on the solid−liquid equilibrium thermodynamics. To determine if multiple solid soap phases were present, the structures of the solid phases were characterized by wide-angle X-ray scattering, FTIR, and DSC. It was found that a single mixed crystalline solid phase is formed over most of the composition range. The bilayer spacing of the soap crystals is close to that of the majority component, except when the weight fractions are roughly equal, in which case the solid phase is largely disordered. The water content of the soap crystals was found to increase continuously with increasing environmental humidity, indicating that soap hydrates are not stoichiometric.

Introduction

Soaps are a class of surface active materials derived from natural oils and fats. Soap molecules are amphiphilic and consist of a polar headgroup and a nonpolar tail, which causes their preference for assembly into sheetlike structures, with the hydrophobic groups on one side and the hydrophilic groups on the other side. The curvature of the interface at which an amphiphilic molecule adsorbs preferentially depends on temperature, composition, and the relative sizes of the head and tail groups.[1] Molecules with small tails and large heads tend to form spherical micellar aggregates, in which the headgroups are located on the outside, shielding the tails inside the micelle. Larger tail groups lead to formation of cylindrical or lamellar micelles, while inverted micelles, in which the heads are in the center and the tails on the outside, tend to be formed in oily solvents when the tail is large and the headgroup small.

The geometry of micelles in aqueous solution depends on the headgroup and tail group sizes as well as on the amphiphile concentration, temperature, and the presence of dissolved salt. The temperature-composition phase diagram of water-soluble surfactants is characterized by a solubility boundary known as the Krafft boundary.[2] Along the Krafft boundary, the surfactant solubility increases slowly as the temperature is increased, until a certain temperature range is reached. Above this temperature range the Krafft boundary forms a plateau, indicating a rapid solubility increase. The homogeneous phase above the Krafft plateau is a micellar solution at low surfactant concentrations. At high concentrations, the Krafft boundary ends and hexagonal or lamellar liquid crystals may exist. The phase behavior in a three-component system is still more complex, since the solubilization capacity of the micelles and mesophases comes into play. Oil-continuous and water-continuous microemulsions can be present, and bicontinuous phases have been observed also.

The oldest type of man-made surfactants, soaps are prepared from natural oils and fats by the saponification process. Because they are synthesized from natural products, they contain a mixture of hydrocarbon chain lengths with an even number of carbon atoms. The phase behavior of the components of commercial soaps has been studied extensively, although few studies have appeared recently in the open literature. Phase diagrams of soaps mixed with the corresponding fatty acids and water have been published for soaps with a chain length n_c (not counting the headgroup) up to that of stearate and oleate (both with $n_c = 17$).[3−6] Longer-chain soaps such as arachidate ($n_c = 19$) and behenate ($n_c = 21$) have largely escaped attention. In addition, while most industrial products contain a mixture of different soaps, with few exceptions the properties of mixed soap phases have not been studied.

* To whom correspondence should be addressed.
† University of Minnesota.
‡ Current address: The Gillette Co., 1 Gillette Park 7G-1, Boston, MA 02127.
§ Imation Corp.

(1) Evans, D. F.; Wennerström, H. *The Colloidal Domain*; VCH Publishers: New York, 1994.
(2) Krafft, F.; Wiglow, H. *Ber. Dtsch. Chem. Ges.* **1895**, *28*, 2573.
(3) McBain, J. W.; Vold, R. D.; Frick, M. *J. Phys. Chem.* **1940**, *44*, 1013.
(4) Luzatti, V.; Mustacchi, H.; Skoulios, A. *Faraday Soc. Discuss.* **1958**, *25*, 43.
(5) Madelmont, C.; Perron, R. *Colloid Polym. Sci.* **1976**, *254*, 581.
(6) Laughlin, R. G. *The Aqueous Phase Behavior of Surfactants*; Academic Press: San Diego, CA, 1994.

10.1021/la000467n CCC: $19.00
Published on Web 09/28/2000

Pure long-chain soaps exist at room temperature as anhydrous crystals or crystal hydrates, depending on the humidity. Whether soaps form stoichiometric hydrates has not been resolved conclusively (ref 6, p 199). However, X-ray diffraction and calorimetric studies show evidence for the existence of a number of different hydrated soap phases for a given chain length. In addition to the anhydrous crystalline soap phase, which is stable only in the complete absence of water, up to three polymorphic hydrated phases may exist in equilibrium.[7−9] When heated, the soap hydrates decompose into a liquid crystalline phase and a different hydrate or the anhydrous soap. Pure anhydrous soaps undergo a sequence of phase transitions, from the crystalline solid through several liquid crystalline phases to the isotropic liquid phase.[5,10,11] The liquid crystalline structure is built up from lamellae or packed flexible rods, depending on the temperature.[12,13]

Binary phase diagrams of soap−water systems have been well established for the most widely used soaps. At low soap weight fractions, the phase behavior as a function of temperature is defined by a Krafft plateau, below which hydrated soap crystals coexist with a dilute aqueous solution. Above the plateau a micellar solution is formed. No information on the micellar shape or size is available, but the critical micelle concentrations of some soaps and soap mixtures have been reported.[14−16] Measurement of the properties of dilute soap solutions is complicated by the appearance of acid soaps produced by soap hydrolysis. These are insoluble phase compounds formed by association of soap ion pairs with one or more molecules of the corresponding fatty acids.[17−19] To make phase observations on dilute soap solutions, the solution pH has to be adjusted to minimize acid soap formation while not affecting the phase behavior.

In summary, the phase behavior of the most widely used soap materials has been well developed. However, many details remain to be worked out. Few recent forays into this field have been made, in particular into the microstructure of the various phases, the properties of mixed soaps, and those of longer chain soaps.

In this paper we report on the phase behavior and microstructure of mixtures of sodium stearate, arachidate, and behenate in aqueous solution. This work was motivated by the need to understand the behavior of aqueous solutions of long-chain soaps used to make silver soaps. The main constituent of thermally developed photographic materials, silver soaps are typically precipitated from sodium soap solutions by adding silver nitrate.[20] Good control of the precipitation process is not possible in the absence of knowledge on the soap solubility and microstructure as a function of the processing conditions. We will show that the properties of aqueous soap solutions and solid soap phases strongly depend on the temperature and soap composition.

Experimental Section

Soap Synthesis. Sodium soaps were prepared from the corresponding fatty acids by neutralization of solutions in ethanol using sodium hydroxide. Palmitic acid (hexadecanoic acid), stearic acid (octadecanoic acid), arachidic acid (eicosanoic acid), and behenic acid (docosanoic acid) were supplied at 99% purity (Aldrich, Milwaukee, WI) and used as received. The fatty acid was dissolved in boiling absolute ethanol, and a stoichiometric amount of sodium hydroxide (99.99% pure, Aldrich) dissolved in an ethanol−water mixture (3:1 by volume) was added dropwise, so that the sodium soap precipitated. Ethanol and water were driven off under vacuum, and the product was dried in a vacuum oven at 105 °C while monitoring its weight. The oven was heated slowly to prevent oxidation. The resulting anhydrous sodium soap was recrystallized from absolute ethanol to remove unreacted fatty acid. After drying, a fine white powder was obtained, which was kept in a desiccator with calcium sulfate as the desiccant. The soaps thus prepared were sodium palmitate (NaPa), stearate (NaSt), arachidate (NaAr), and behenate (NaBe).

Hydrated soap crystals were made by equilibrating the soaps in a controlled humidity atmosphere over saturated salt solutions. The salts used were potassium acetate (20% humidity at room temperature), calcium nitrate (50%), and zinc sulfate (90%).[21] The hydrated soap crystals were allowed to equilibrate for 3 weeks or more until their weight remained constant. The amount of hydrated water after equilibration was determined by Karl Fischer titration.

Fourier Transform Infrared Spectroscopy (FTIR). A check on the soap purity was provided by FTIR measurements. For this purpose a Nicolet Magna 750 FTIR spectrometer with attenuated total reflectance (ATR) attachment was used. The ATR attachment served to minimize the amount of water introduced into the sample by the sample preparation process. Each spectrum recorded was the sum of 32 consecutive measured spectra, corrected for the background spectrum obtained in air. No absorption peaks due to water or fatty acid were observed for the anhydrous soaps, while hydrated soaps exhibited a broad weak absorption band at 3400 cm^{-1} caused by the hydrating water molecules.

Karl Fischer Titration. The extent of hydration for the various hydrated soap crystals was measured by Karl Fischer titration using a Photovolt Instruments Aquatest CMA Karl Fischer coulometric titrator (UMM Electronics, Indianapolis, IN). Pyridine-free Karl Fischer reagents supplied by Photovolt Instruments were used. Water was extracted from the soap crystals by dispersing a measured amount in a known quantity of methanol and allowing for equilibration. The methanol solvent was ACS grade and was dried with 3A molecular sieves. In the calculation of the water fraction in the hydrated soap, the amount of water remaining in the dry methanol was taken into account.

Differential Scanning Calorimetry (DSC). To verify the visual phase behavior observations and to detect solid-phase transitions, DSC scans were obtained on the pure anhydrous soaps and on aqueous soap solutions. For this purpose a Perkin-Elmer DSC 7 differential scanning calorimeter was used. The samples were contained in aluminum sample pans, which were sealed by O-rings so that larger than atmospheric pressures were feasible. This made it possible to heat anhydrous samples to 300 °C and aqueous samples to about 220 °C. The instrument was calibrated by setting the onset temperature of the melting peak of pure indium to the literature value, and the precision of the temperature reading was ±0.1 °C.

Phase Behavior Observations. Isoplethal (constant composition) phase behavior studies of sodium soap mixtures in aqueous solution were carried out by visual observation of the phases present in mixtures of known composition as a function of temperature. Mixed soap solutions were made up by weight and heated while stirred in closed test tubes at 90 °C or higher

(7) Ferguson, R. H.; Rosevear, F. B.; Stillman, R. C. *Ind. Eng. Chem.* **1943**, *35*, 1005.
(8) Buerger, M. J.; Smith, L. B.; Ryer, F. V.; Spike, J. E., Jr. *Proc. Natl. Acad. Sci. U.S.A.* **1945**, *31*, 226.
(9) Perron, R. *Rev. Fr. Corps. Gras.* **1976**, *23*, 473.
(10) Vold, M. J.; Macomber, M.; Vold, R. D. *J. Am. Chem. Soc.* **1941**, *63*, 168.
(11) Small, D. M. *The Physical Chemistry of Lipids, From Alkanes to Phospholipids;* Handbook of Lipid Research, Vol. 4; Plenum Press: New York, 1986; Chapter 9.
(12) Skoulios, A. E.; Luzzati, V. *Acta Crystallogr.* **1961**, *14*, 278.
(13) Luzzati, V. In *Biological Membranes, Physical Fact and Function*; Chapman, D., Wallach, D. F. H., Eds.; Academic Press: New York, 1968; p 71.
(14) Corrin, M. L.; Harkins, W. D. *J. Am. Chem. Soc.* **1947**, *69*, 683.
(15) Klevens, H. B. *J. Phys. Chem.* **1948**, *52*, 130.
(16) Shinoda, K. *J. Phys. Chem.* **1954**, *58*, 541.
(17) McBain, J. W.; Field, M. C. *J. Am. Chem. Soc.* **1933**, *55*, 4776.
(18) Ekwall, P. *Kolloid-Z.* **1937**, *80*, 77.
(19) Lynch, M. L.; Pan, Y.; Laughlin, R. G. *J. Phys. Chem.* **1996**, *100*, 357.
(20) Simons, M. J. U.S. Patent 3,839,049, 1972.
(21) *Handbook of Chemistry and Physics*, 51st ed.; Weast, R. C., Ed.; CRC: Cleveland, OH, 1970.

for homogenization. They were then slowly cooled to room temperature, leading to precipitation of hydrated soap crystals. Water used was distilled and filtered by a Millipore filtration unit. It contained 10^{-4} M NaOH to prevent soap hydrolysis and subsequent formation of acid soap crystals, which make the solutions cloudy, particularly for samples containing NaBe. This concentration is the highest possible without significantly affecting the experimental results. The clearing temperature T_c, which is the temperature at which the last crystal dissolves, was determined by very slowly heating each sample in a thermostatic bath (0.2 °C/5 min near T_c). Above the clearing temperature solutions are isotropic and highly viscous above 5 overall soap wt %. On occasion two apparently separate liquid phases were observed. However, these observations were not reproducible and can be ascribed to bad mixing and very slow equilibration of the soap−water mixtures.[22]

Fluorescence Spectroscopy. The cmc of surfactants was measured by fluorescence spectroscopy using pyrene (Aldrich) as the fluorescent probe. The spectrum of pyrene depends strongly on the polarity of the molecular environment. If micelles are formed in an aqueous solution, the nonpolar pyrene molecules will transfer from the bulk solution to the micellar core. This leads to an increase in the intensity ratio of peaks I and III in the pyrene fluorescence spectrum.[23] We measured the cmc of the sodium soaps as a function of temperature by incrementally increasing the temperature of a solution of known composition, recording the pyrene fluorescence spectrum, and afterward plotting the III to I peak intensity ratio as a function of temperature. The point at which the III/I ratio undergoes a step change was taken as a measure of the cmc. The time allowed for equilibration between spectra was 30 min, and three spectra were recorded at each temperature. Solutions contained 10^{-4} M NaOH to reduce soap hydrolysis unless otherwise mentioned. Samples were prepared by first allowing a dilute solution of pyrene in *n*-hexane to dry in a small flask and then adding soap and water in the desired amounts, heating until the soap dissolved, and pipetting a few mL of solution into a quartz fluorescence cuvette. The molar ratio of pyrene to soap was less than 10^{-3}, so that only a fraction of micelles contained probe molecules, unless the micelles were unexpectedly large. The cuvettes were held in a custom built insulated cuvette chamber with internal heating coils through which water from a thermostatic water bath was circulated. A thermocouple was located in the chamber within a few centimeters of the cuvettes.

X-ray Diffraction. Wide-angle X-ray diffraction studies were done on the mixed soap crystals to determine to what extent the different soaps mix in the solid phase and to measure the bilayer spacings of the mixed soap crystals as a function of composition. The instrument used was a Scintag diffractometer equipped with a high-temperature attachment. Samples were prepared as for the phase behavior studies and were contained in a copper sample holder closed to the environment by a thin Kapton polyimide film. Best results were obtained without drying the crystals, and therefore, the results shown correspond to the hydrated soap phase. Excess water was removed from the soap crystals by pressing them between a glass microscope slide and a filter paper. In most cases, at least the first five diffraction orders corresponding to the bilayer spacing could be observed and the spacing calculated by averaging the spacings deduced from each peak.[24]

Results

Solution Phase Behavior. The phase behavior of the pure sodium soaps at high water content was determined by measurement of the soap solubility in aqueous solutions as a function of temperature. The Krafft boundary has its characteristic knee and plateau form (Figure 1). As a single characteristic of the Krafft boundary, a Krafft point can be defined as the temperature at which the solubility equals 1 wt %.[6] The Krafft point increases linearly with

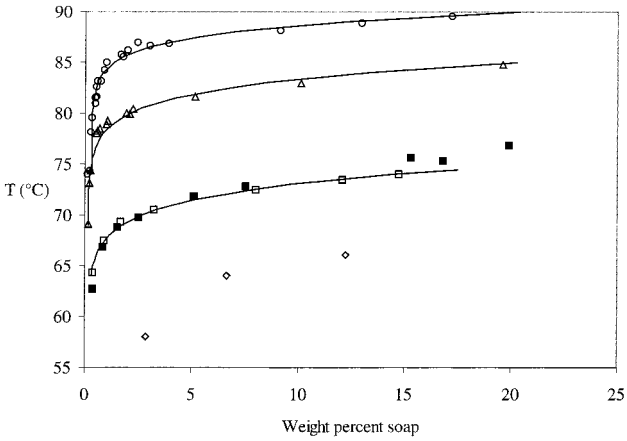

Figure 1. Krafft boundaries of long-chain sodium soaps in aqueous solution. Data shown are for NaPa (◇ from ref 25), NaSt (□; ■ from ref 3), NaAr (△), and NaBe (○). The curves are results from eq 8.

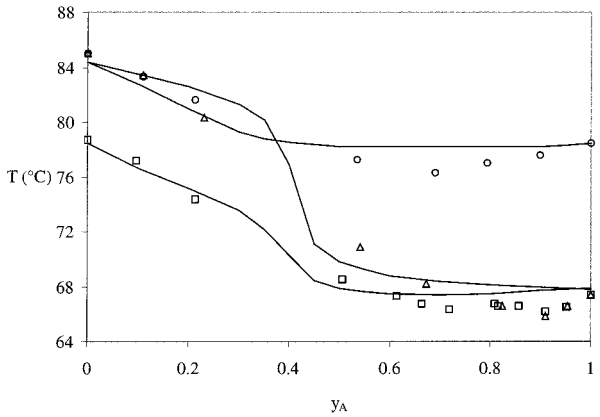

Figure 2. Krafft points of mixtures of two soaps in aqueous solution. Data for NaSt/NaAr (□), NaSt/NaBe (△), and NaAr/NaBe (○). The curves are results from eq 15.

the alkyl chain length of the soap. Below the Krafft point, the solubility increase with temperature is slow. Once the knee in the solubility is reached, the solubility increases more rapidly, until a liquid crystalline region in the phase diagram is encountered (not shown). Our results for NaSt closely reproduce results obtained by McBain et al. using similar visual observations.[3,25]

Above the Krafft boundary, the system is an isotropic solution of the soap in water. Below the boundary, soap crystals coexist with the solution phase. The structure of the crystalline phase will be discussed in detail below. At low soap concentrations, the isotropic solution is cloudy due to formation of acid soaps caused by soap hydrolysis. Although the alkalinity of the soap solution was increased by adding base to suppress hydrolysis, at very low concentrations acid soaps were still observed, especially for NaAr and NaBe.

The phase behavior of mixtures of two and three soaps in solution was studied by measuring the Krafft point vs the mixture composition (Figures 2 and 3). In all cases a minimum Krafft point exists which is lower than the Krafft points of the constituent soaps. The minimum is located at a high mass fraction of the lowest chain length component soap. Mixtures of soaps can thus be more soluble than pure soaps. The minimum is not a eutectic discontinuity, as reported in mixtures of other anionic

(22) Flecker, O. J.; Taylor, M. *J. Chem. Soc.* **1922**, *121*, 1101.
(23) Kalyanasundaram, K.; Thomas, J. K. *J. Am. Chem. Soc.* **1977**, *99*, 2039.
(24) Chapman, D. *The Structure of Lipids, by Spectroscopic and X-Ray Techniques*; Methuen and Co. Ltd.: London, 1965.
(25) McBain, J. W.; Lazarus, L. H.; Pitter, A. V. *Z. Phys. Chem.* **1930**, *A147*, 87.

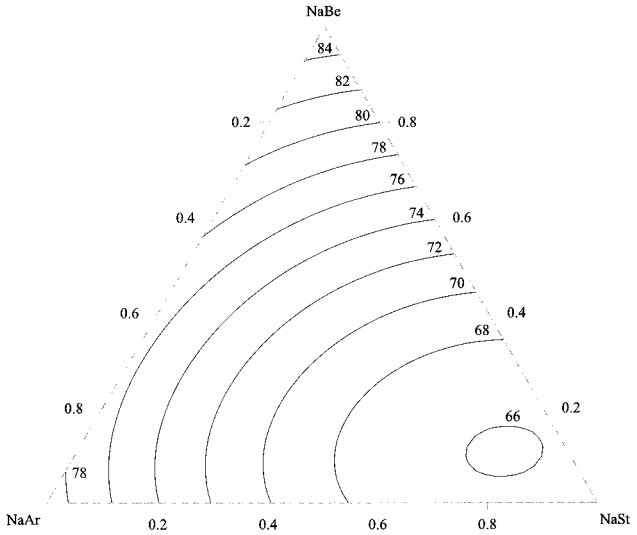

Figure 3. Krafft points of mixtures of three soaps in aqueous solution. The data are represented by isotherms obtained by fitting the points to a polynomial.

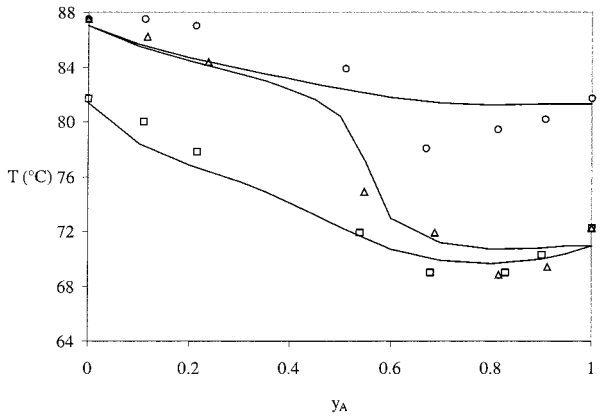

Figure 4. Solubility boundary temperatures of mixtures of two soaps in aqueous solution at 4 wt %. Data for NaSt/NaAr (△), NaSt/NaBe (◇), and NaAr/NaBe (□).

surfactants.[26] This indicates that solid soap crystals may be partially miscible. Similar behavior is observed in the temperature of the solubility boundary of two and three soap mixtures at 4 wt % (Figures4 and 5).

Critical Micelle Concentrations. Data for the critical micelle concentrations of the long-chain soaps were obtained by fluorescence microscopy using pyrene as the probe molecule. As mentioned before, on increase of the soap solution temperature, the ratio between peaks III and I in the pyrene fluorescence spectrum shifts to higher values when the cmc is reached (Figure 6). The shift in the peak ratio occurs in a narrow temperature range, indicating that the cmc is sharp. The temperature at which the shift takes place was plotted against the solution composition to obtain the temperature dependence of the cmc (Figure 7).

As apparent from the figure, the reproducibility of the data is not very good, especially for NaAr. Poor reproducibility was caused by the presence of acid soap, by poor mixing of the solutions in the cuvettes, and by the location of the thermocouple at some distance from the cuvettes. Due to these difficulties, data collection for NaBe was problematic, and the results for NaBe are only shown in the figure to indicate the approximate height and slope of the cmc vs temperature curve.

(26) Hato, M.; Shinoda, K. *J. Phys. Chem.* **1973**, *77*, 378.

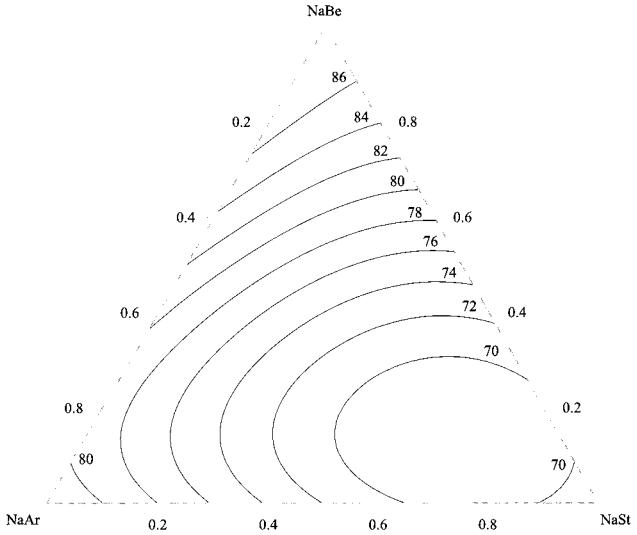

Figure 5. Solubility boundary temperatures of mixtures of three soaps in aqueous solution at 4 wt %. The data are represented by isotherms obtained by fitting the points to a polynomial.

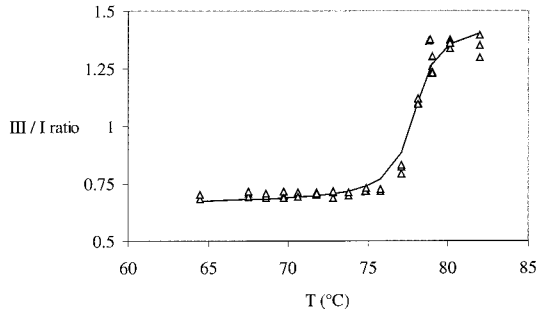

Figure 6. Ratio between peaks III and I in the pyrene fluorescence spectrum vs temperature for a 0.17 wt % NaAr solution. The continuous line is a fitted curve based on the arctangent function.

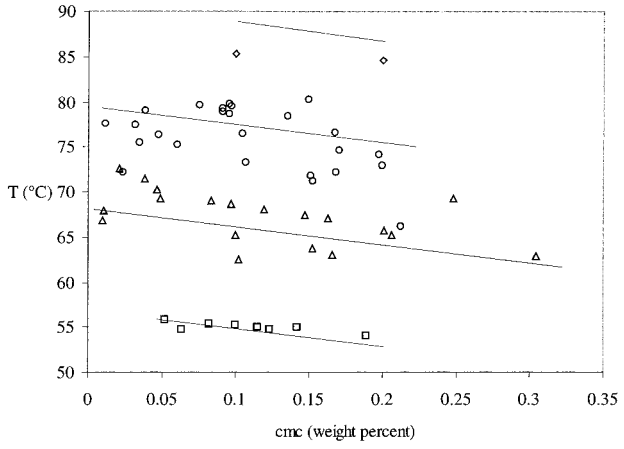

Figure 7. Critical micelle concentrations of long-chain sodium soaps vs temperature measured by fluorescence spectroscopy. Data are for NaPa (□), NaSt (△), NaAr (○), and NaBe (◇). The curves are obtained by fitting eq 2, except for NaBe.

For all soaps, the cmc intersects the solubility boundary between 0.2 and 0.4 wt %, well below the knee of the Krafft boundary and below the 1 wt % solubility chosen before as the Krafft point. The cmc decreases rapidly and linearly when temperature increases. The high temperature dependence of the cmc contrasts with the low temperature dependence observed in other surfactants.[27,28]

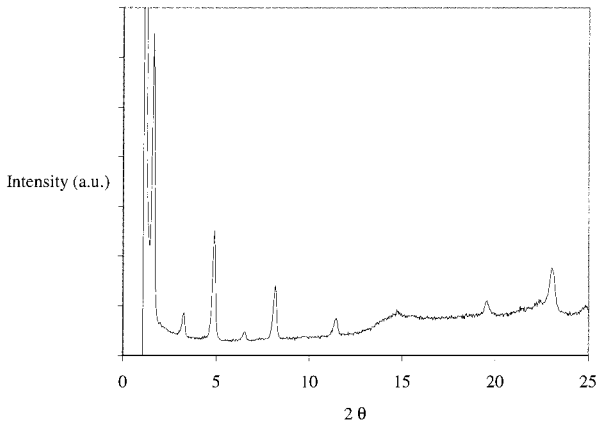

Figure 8. WAXS pattern of hydrated NaBe. Low scattering angle peaks give information on the bilayer spacing, and high-angle peaks are due to the crystalline arrangement of the hydrocarbon chain segments. The broad scattering band between 15 and 30 deg stems from the polyimide film used to contain the sample.

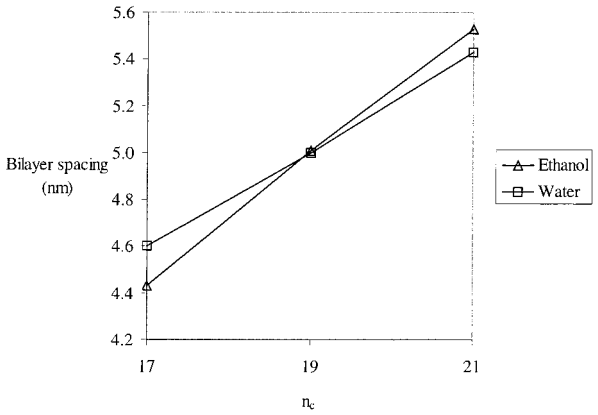

Figure 9. Bilayer spacing of soap crystals measured by WAXS vs soap chain length. The slope of the curves can be used to calculate the hydrocarbon chain tilt angle within the bilayers; see text. Data shown are for anhydrous soaps, crystallized from ethanol, and for hydrated soaps, crystallized from water.

Solid-Phase Composition and Structure. To determine to what extent the soaps mix in the solid phase, WAXS data were obtained on pure soaps and on mixtures of two soaps. As mentioned before, the soap solids were crystallized from an aqueous solution and not completely dried. This method of preparing the samples gave the most intense scattering peaks. As an example, the scattering pattern of pure NaBe is given in Figure 8. The strongest peak in the pattern is the first-order bilayer peak at about $2\theta = 1.5°$. Subsequent peaks alternate in intensity while the average intensity decreases. These are higher-order reflections from the bilayers. The mean bilayer spacing is calculated by averaging the bilayer spacings derived from each of the peaks using Bragg's law. The standard deviation of the resulting value indicates the amount of noise in the data, and this may be used to gauge the degree of crystallinity of the soap solids. The two peaks at scattering angles $2\theta = 19.5°$ and 23.0° correspond to the crystalline arrangement of the hydrocarbon chain segments. These reflections disappear when the soap enters an isotropic or liquid crystalline phase. Note also that the broad band above $2\theta = 15°$ is caused by the polyimide film used to confine the soap crystals.

By plotting the bilayer spacing against the soap chain length, an estimate of the tilt angle of the hydrocarbon chains with the bilayer plane can be obtained. This is done by fitting a straight line through the data and determining the slope (Figure 9). We found that the slope is 0.274 nm for anhydrous soaps and 0.206 nm for hydrated soaps. Since the distance between adjacent carbon atoms parallel to the chain is 0.126 nm,[24] the chain tilt angle for the hydrated soaps would be 54.8°. A somewhat higher value of 67.9° at 20 °C has been reported for silver soaps.[29] For the anhydrous soaps, however, the increase in bilayer spacing is larger than expected on the basis of the chain length increase, so that a tilt angle cannot be computed. This result casts doubt on the value of the tilt angle for hydrated soaps as well, and further work is necessary to determine the molecular arrangement in the solid phase.

To determine the microstructure of mixed solid soap phases, the bilayer spacing was measured for mixtures of two soaps (Figure 10). If the two soaps form two separate crystalline phases with a different bilayer spacing, each scattering peak would appear as a doublet. Instead, in most cases a single crystalline phase is detected, indicating that two soaps form mixed crystals over a large part of the composition range. When the mixture contains approximately equal quantities of each soap, the crystal phase becomes more disordered, leading to less well-defined peaks and larger standard deviations (indicated by the error bars). For NaAr/NaBe mixtures (Figure 10c), two separate crystalline phases are formed between 30 and 70 wt % NaAr, which are not observed in the other mixtures (Figure 10a,b). These phases are both mixtures of NaAr and NaBe but presumably have different compositions. Similarly, the disordered crystals formed in 50 wt % NaSt/NaBe have some tendency to demix but not as clearly as in NaAr/NaBe mixtures. Phenomena analogous to these were observed in mixtures of three soaps.

Stability of Crystal Hydrates. The properties of the solid soap phase depend on the amount of water contained in the soap crystals. To determine to what extent water is absorbed by the soaps as a function of the humidity of the surrounding air, soap crystals were equilibrated with various humidity levels, and the water content was measured by Karl Fischer titration. The results are represented in Figure 11. For all soaps, the water mole fraction in the solid phase increases with the humidity of the environment in similar fashion. We observe that the bulk of the water is already absorbed at a low humidity level, and the water mole fraction increases for each subsequent increase in humidity. Therefore, water does not absorb in one or two distinct stoichiometric ratios. On the basis of this observation, we believe that the solid phases consist not of hydrated crystals with a distinct stoichiometry but of swollen crystals with a smoothly variable amount of absorbed water.

Figure 11 also indicates that NaSt and NaAr solids contain approximately equal amounts of water at equilibrium at all humidity levels. Perhaps contrary to expectations based on the increased overall hydrophobic character of the solid phase, NaBe crystals absorb slightly more water, about 5 mol % more, than the other soaps. This observation may be rationalized by noting that most hydrated water molecules are located between the bilayers formed by the soap molecules, close to the hydrophilic headgroups. A small increase in the crystalline spacing between the headgroups could easily account for the difference between NaBe and the other two soaps studied.

(27) Kresheck, G. C. In *Water, a comprehensive treatise*; Franks, F., Ed.; Plenum: New York: 1975; Vol. 4, p 95.
(28) La Mesa, C. *Colloids Surf.* **1989**, *35*, 329.
(29) Vand, V.; Aitken, A.; Campbell, R. K. *Acta Crystallogr.* **1949**, *2*, 398.

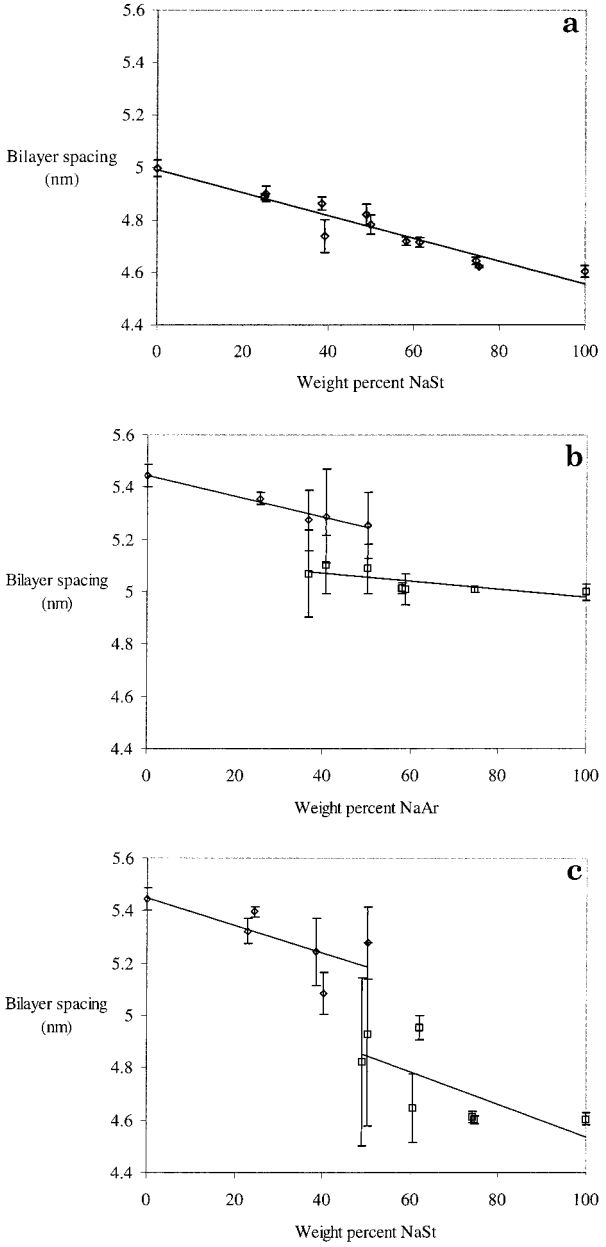

Figure 10. Bilayer spacings of hydrated mixtures of two soaps vs composition as measured by WAXS. Composition is indicated by the weight fraction of the lower chain length component in NaSt/NaAr (a), NaSt/NaBe (b), and NaAr/NaBe (c) mixtures. Error bars are the standard deviations in the spacing values.

While different soap crystalline phases could potentially contain more water, no evidence for the existence of such phases below the Krafft temperature was found by DSC. Differential calorimetric scans of 5, 10, and 15 wt % NaSt crystals in water show a single absorption peak, as shown in Figure 12. Note that the heat axis in this figure has been normalized with respect to the mass of soap in each sample. The peaks for different soap weight fractions largely overlap. Moreover, the onset of the peaks occurs a few degrees lower than the clearing point, and the peaks are not symmetric. Indeed, the peaks do not reflect a sharp phase transition but a gradual dissolution process until the boundary of the coexistence region of soap solids and aqueous solution is reached. The onset of the peaks indicates the point at which the Krafft temperature of the soap is reached. At this point, which is relatively sharp, the soap solubility increases rapidly on raising the temperature, leading to a large latent heat consumption.

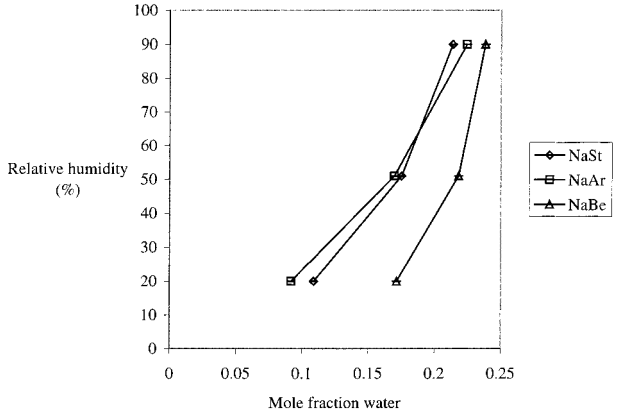

Figure 11. Equilibrium water content of single soaps determined by Karl Fischer titration vs relative humidity.

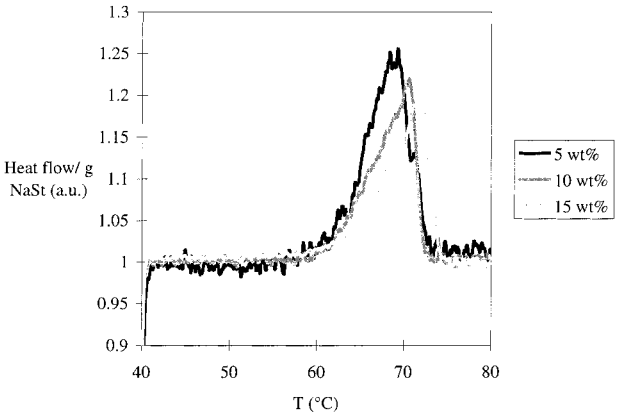

Figure 12. DSC results for NaSt as a function of weight fraction in water.

The end point of the peak may be taken as a measure for the clearing point.

Discussion

Single Soap Solutions. The knee and plateau structure of the soap solubility boundary is commonly observed in surfactant solutions. The rapid increase in solubility as the temperature exceeds the Krafft point has been ascribed to the formation of micelles. Often, the temperature at which the cmc vs temperature curve and the Krafft boundary intersect is close to the knee. In this view, the formation of surfactant micelles is akin to a phase separation process, in that the capacity of the solution for soap molecules is much increased. In contrast, the cmc data for the long-chain soaps studied here indicate that the cmc intersects the Krafft boundary at temperatures much lower than the knee. Therefore, micelles are present at the entire boundary except at very low soap concentrations. For these materials, the location of the Krafft point is not related to the occurrence of micelles. Indeed, it has been observed that knees and plateaus are not unique to the solubility boundaries of surfactant systems, which further weakens the link between the cmc and the knee.[6]

Alternatively, the Krafft point may be related to a melting phenomenon in the solid soap.[30] The locations of the knees in the solubility boundaries of the soaps are fairly close to the melting points of the corresponding fatty acids. However, the pure soaps form an isotropic liquid only at much higher temperatures, and even the phase transition from the soap crystal to the first subwaxy phase

(30) Shinoda, K.; Hato, M.; Hayashi, T. *J. Phys. Chem.* **1972**, *76*, 909.

Table 1. Values of Parameters Used to Fit the Dependence of the cmc on Temperature

parameter	value (K)
p_1	−2006
p_2	0
p_3	5.7
p_4	244

occurs above 100 °C.[3,5,17] Therefore, if a phase transition in the solid phase takes place at the Krafft point, the soap crystals must have a structure different from that of the anhydrous crystalline soap. No evidence for such a structure was present in our WAXS observations.

The rapid increase in soap solubility just below the Krafft boundary is reproduced in the DSC analysis results of NaSt solutions. No solid-phase transitions in the soap crystals are observed until 60 °C, when soap starts to dissolve at an increasing rate until all is in solution. The dissolution process is similar to a melting transition in the sense that the transition is sharp and initiated at a reproducible temperature. However, in contrast to melting points, dissolution continues over a range of temperatures until the Krafft boundary is reached. Whether this process is a true phase transition, involving a molecular rearrangement in the solid phase, remains to be determined.

Temperature Dependence of the cmc. The cmc data measured by fluorescence microscopy show a dependence of the cmc on temperature and on soap chain length. For higher chain length soaps, the cmc vs temperature curve shifts to higher temperatures, similar to the Krafft boundary. This dependence of the cmc on chain length has been observed in other surfactants, but the temperature dependence is unusual.[27,28] The cmc decreases strongly with small increases in temperature for the long-chain sodium soaps tested. In contrast, an opposite slope of the cmc vs temperature curve has been reported in potassium laurate and myristate soaps.[15] The lower chain length potassium soaps exhibited a cmc that increased with temperature.

This seemingly inconsistent behavior may be reconciled by the observation that many surfactants have a minimum cmc at a certain temperature.[27] Therefore, the cmc data of the soaps reported here and in the literature may represent different legs of the cmc vs temperature curve. If a minimum exists in the curve for the long chain sodium soaps, it is inaccessible as it would fall below the Krafft boundary.

Because of the scatter in the experimental cmc data, a linear function was used to fit the data:

$$T = A + B(\text{cmc}) \tag{1}$$

The fitting parameters A and B were found to depend linearly on the soap chain length, leading to the fitting equation

$$T = (p_1 n_c + p_2)\text{cmc} + p_3 n_c + p_4 \tag{2}$$

We found that the value of p_2 equaled zero to a good approximation. Values for the parameters p_1, p_3, and p_4 are given in Table 1. These parameters were fitted to the data for NaPa, NaSt, and NaAr only. The cmc vs temperature curve of NaBe is predicted fairly well.

Soap Solubility Model. The characteristic shape of the Krafft boundaries of the soaps can be reproduced by a thermodynamic model, on the basis of the assumption that the soap micelles may be regarded as a separate phase. The micelles will have a certain size distribution, which is determined by the dependence of the soap chemical potential in the micelle μ_n^0 on the aggregation number n. For the purposes of this study, it is assumed that the micelles are spherical and monodisperse. A value for n may then be calculated on the basis of the soap hydrocarbon chain length l_c and volume v_c:

$$n = \frac{4}{3}\pi {l_c}^3/v_c \tag{3}$$

Values for n are in Table 2.

Table 2. Modeling Results for Krafft Boundaries of Pure Soaps

soap	n	cmc × 10^6 (mole fraction)	ΔH_{tp} (kJ/mol)	T_{tp} (K)
NaPa	84			
NaSt	106	85	459	368.7
NaAr	131	76	530	377.6
NaBe	158	143	678	379.1

Free energy minimization leads to the following expression for the mole fraction x_n of micelles in the solution:

$$x_n = {x_1}^n \exp\left(-\frac{\mu_n^0 - n\mu_1^0}{kT}\right) \tag{4}$$

Here x_1 is the monomer mole fraction and μ_n^0 and μ_1^0 are the chemical potentials of the micelles and monomers, respectively.

Assuming a phase separation model for micellization,[31]

$$\frac{\mu_n^0}{n} = \mu_1^0 + kT \ln \text{cmc} \tag{5}$$

Combining

$$x_n = \left(\frac{x_1}{\text{cmc}}\right)^n \tag{6}$$

For large n, as is the case for long-chain soaps, the monomer concentration is less than but very close to the cmc if eq 6 is satisfied. We may assume that the monomer concentration is approximately equal to the cmc when the total soap concentration is above the cmc.

A version of the general solubility equation applied to the micelles only is[32]

$$x_n = \frac{1}{\gamma_n} \exp\left[\frac{\Delta H_{tp}}{R}\left(\frac{1}{T_{tp}} - \frac{1}{T}\right)\right] \tag{7}$$

In this equation ΔH_{tp} and T_{tp} are the enthalpy of solution and the temperature at the triple point. We will use these properties as fitting parameters. Assuming the activity coefficient is 1, for micelles and monomers

$$x_{soap} = \text{cmc} + n \exp\left[\frac{\Delta H_{tp}}{R}\left(\frac{1}{T_{tp}} - \frac{1}{T}\right)\right] \tag{8}$$

The temperature dependence of the cmc may be substituted from eq 2, but this would involve extrapolation well beyond the measured temperature ranges of the cmc. Therefore, the cmc was taken as a third fitting parameter. As shown in Figure 1, eq 8 fits the Krafft boundaries well. Parameters cmc, ΔH_{tp}, and T_{tp} are listed in Table 2 for the four soaps.

(31) Rubingh, D. N. In *Solution Chemistry of Surfactants*; Mittal, K. L., Ed.; Plenum: New York, 1979; Vol. 1, p 337.
(32) Walas, S. M. *Phase Equilibria in Chemical Engineering*; Butterworth Publishers: Boston, MA, 1985.

Mixed Soap Solutions. A minimum Krafft temperature exists in plots of the Krafft point vs composition in binary and ternary soap mixtures. At and close to the minimum the solubility of the mixture is higher than that of the individual components. Minima in the Krafft point have been observed before in mixtures of various surfactants.[26,30] In those instances, the phenomenon was thought to be analogous to freezing point depression. The analogy may apply here also, although the minimum is a shallow trough for the soaps as opposed to a sharp inverted peak.

The features of the Krafft temperature vs composition curve for mixtures of two soaps can be reproduced with a thermodynamic model. For a soap A, thermodynamic equilibrium between the solid and the solute is given by

$$\mu^0_{A,s} + RT \ln a_{A,s} = \mu^0_{A,l} + RT \ln a_{A,l} \tag{9}$$

Here $a_{A,s}$ and $a_{A,l}$ are the activities of soap A in the solid and liquid phases and $\mu^0_{A,s}$ and $\mu^0_{A,l}$ the corresponding standard chemical potentials. The exact choice of standard states for $\mu^0_{A,s}$ and $\mu^0_{A,l}$ is not important here, because the standard chemical potentials will be eliminated in the following analysis.

For a pure soap $a_{A,s} = 1$ and eq 9 becomes, with $a^*_{A,l}$ the activity in a pure soap solution,

$$\mu^0_{A,s} = \mu^0_{A,l} + RT \ln a^*_{A,l} \tag{10}$$

Because the solutions are dilute, we may assume that the activity coefficients in the liquid phase are equal to 1. Therefore, we can replace the activities with the mole fractions:

$$\mu^0_{A,s} = \mu^0_{A,l} + RT \ln x^*_{A,l} \tag{11}$$

The water concentration in the solid phase is assumed to be negligible. For a mixture of two soaps, A and B, the following then obtains from eqs 9 and 11, writing the activity of each in the solid phase as the product of the mole fraction and the activity coefficient:

$$x^*_{A,l}\gamma_{A,s}x_{A,s} = x_{A,l} \tag{12a}$$

$$x^*_{B,l}\gamma_{B,s}(1 - x_{A,s}) = x_{B,l} \tag{12b}$$

For the systems studied here, the mole fraction of water in the solution, x_w, is known. Using eqs 12a,b

$$x_w = 1 - x^*_{A,l}\gamma_{A,s}x_{A,s} - x^*_{B,l}\gamma_{B,s}(1 - x_{A,s}) \tag{13}$$

Solving for $x_{A,s}$

$$x_{A,s} = \frac{1 - x_w - x^*_{B,l}\gamma_{B,s}}{x^*_{A,l}\gamma_{A,s} - x^*_{B,l}\gamma_{B,s}} \tag{14}$$

At the solubility boundary of the mixture, the amount of solid phase is vanishingly small. Using eqs 12a,b and 14, the fraction of soap A in the mixture of A and B, y_A, is then

$$y_A = \frac{x_{A,l}}{x_{A,l} + x_{B,l}} = \frac{\gamma_{A,s}x^*_{A,l}(1 - x_w - \gamma_{B,s}x^*_{B,l})}{(\gamma_{A,s}x^*_{A,l} - \gamma_{B,s}x^*_{B,l})(1 - x_w)} \tag{15}$$

For unit solid-phase activity coefficients, this relation allows calculation of y_A at any temperature, solely based on the pure soap solubilities. However, the observed Krafft temperatures for the mixtures are better described with a simple symmetrical model for the activity coefficients.[32] A fitting parameter A is introduced according to

$$\ln \gamma_{A,s} = A x_{B,s}^2 = A(1 - x_{A,s})^2 \tag{16a}$$

$$\ln \gamma_{B,s} = A x_{A,s}^2 \tag{16b}$$

Applying eqs 16a,b for the activity coefficients and fitting parameter A to the experimental data produces characteristic spoon-shaped curves (Figure 2). Values for the parameter A at different overall soap concentrations are listed in Table 3.

Table 3. Modeling Results for Mixtures of Two Soaps

soap mixture	A (1 wt % tot. soap)	A (4 wt % tot. soap)
NaSt/NaAr	2.5	3.3
NaAr/NaBe	2.1	2.5
NaSt/NaBe	1.4	2.4

The unusual shape of the fitting curves is due to the shape of the Krafft boundary reflected in $x^*_{A,l}$ and $x^*_{B,l}$ and to the dependence of $\gamma_{A,s}$ and $\gamma_{B,s}$ on the composition in eqs 16a,b. Although the curve shapes do not reflect physical phenomena in the mixed soap solutions, the curves fit the data as well as expected on the basis of a single model parameter. The values of A represent the values of $\ln \gamma_{A,s}$ and $\ln \gamma_{B,s}$ at infinite dilution, where the mole fraction of one of the components approaches zero. Therefore, the model is more accurate near the axes, which represent solutions of the pure soaps. The small dependence of A on the soap concentration indicates imperfections in the model. A significant improvement of the model would require a better understanding of the interactions in the solid phase, so that the chemical potential of the soaps in the mixed solid can be calculated more accurately.

Structure and Composition of Soap Crystals. Soap molecules in pure soap crystals are arranged in bilayers, with their hydrophobic backbones tilted with respect to the bilayer plane. The chain tilt allows the headgroup area to be relatively large while maintaining a constant density of CH_2 groups in the hydrophobic region. As such, it represents a compromise between repulsive electrostatic interactions between the heads and attractive van der Waals forces between the chain segments. Changing either of these effects, for example by using bivalent cations, will change the bilayer spacing.

In earlier studies of shorter chain length soap crystals by single-crystal X-ray diffraction[7,8] and by differential thermal analysis[5,9] it was concluded that those materials form one or more hydrated soap crystals, with a different amount of water molecules incorporated in the crystal structure. The stoichiometry of the most prevalent NaSt hydrate is generally given as $(NaSt)_2 \cdot H_2O$.[8] This composition was stated to have been measured using a distillation technique based on the xylene/water azeotrope. The soap solids used were crystallized from ethanol and water at various temperatures, while the method of equilibration with humid air was not mentioned. In contrast, our Karl Fischer results show no evidence for the existence of a stoichiometric hydrate in any of the soaps studied. The mole fraction of water in equilibrium with a humid atmosphere is far below the 33 mol % required by a $(NaSt)_2 \cdot H_2O$ hydrate. In addition, the water content of the soap crystals increases smoothly with humidity, so that the amount of water taken up by the soap crystals is variable. From these results we conclude that the long-chain soaps form hydrated crystals without a fixed stoichiometry.

Mixed Soap Crystals. On the basis of the values of the solid phase activity coefficients obtained from the

mixed soap model, the solid phases in mixed soaps do not behave as ideal mixtures. This conclusion is supported by the X-ray evidence. A variety of crystalline phases with different bilayer spacings has been observed, which sometimes coexist. The mixed crystals may have three possible structures. First, the crystalline structure can be that of the majority component, with the minority component incorporated in crystalline defects. This is probably the case when the minority component has a mole fraction of less than 30 mol %. In those cases the X-ray scattering peaks are strong and sharp, indicating a well-defined crystal structure.

The second possible crystal structure is a solid solution with a continuously variable composition, with a certain number of defects to incorporate the different chain lengths of the soaps. In this case a single bilayer spacing would be observed even at equal amounts of each soap, as observed in NaSt/NaAr mixtures. The bilayer spacing in those mixtures has an S-shaped dependence on the composition, with a value close to that of the majority component near the axes. In the center of the curve the standard deviation in the measured bilayer spacing is small, which indicates that the scattering peaks are still sharp.

Finally, a large part of the solid phase may have a disordered or amorphous crystal structure. A solid soap with such a structure would not be apparent in the X-ray scattering scan other than as a diffuse band, similar to the scattering band around 15° caused by the polymer film used to confine the soaps. Therefore we can only determine indirectly whether a disordered phase is present. Large uncertainties in the bilayer spacing reflecting weak and broad scattering peaks, for example in NaSt/NaBe mixtures, point to the presence of disordered material. However, even well-defined, strongly scattering crystals may coexist with some disordered material. For that reason the bilayer spacing alone cannot be used to draw conclusions about the composition of the various solid structures.

In the binary soap mixtures, two coexisting crystalline phases were observed in NaSt/NaBe and more clearly in NaAr/NaBe mixtures. If these phases coexist with a disordered phase as well, the ordered phase may consist of pure or nearly pure soaps. However, the bilayer spacing does change significantly when the composition is changed, so that each ordered phase must incorporate a variable amount of the minority soap. In the ternary soap mixture two coexisting crystalline phases have also been observed in a narrow region of the phase diagram. However, because the solid phase consists of three soaps, a small amount of a second or third crystalline phase may only appear as weak shoulders next to the main scattering peaks. For this reason any two-phase regions drawn in the ternary diagram can only be drawn roughly. Finally, as mentioned before, all X-ray measurements were done on solid soap with a large water content. As we have seen that the soap crystals absorb at most 24 mol % water and that the difference in bilayer spacing between hydrated and anhydrous crystals is small (Figure 9), qualitative trends observed in the mixed soap data apply to the anhydrous soaps as well.

Conclusions

The phase behavior of some long-chain sodium soaps in water was studied at low soap weight fractions. The solubility of the soaps in water is determined by a Krafft solubility boundary, below which a micellar soap solution is in equilibrium with solid soap crystals. It was found that the occurrence of a knee in the boundary at the Krafft temperature is not related to the cmc in these systems or to solid-phase transitions. The Krafft boundary is well described by a simple solubility equation for the micelles, which includes the soap cmc as a factor. The cmc decreases when the temperature is raised and increases with an increase in soap chain length. In contrast to literature results, the temperature dependence of the cmc is strong.

The Krafft temperature for mixed soaps was observed to have a minimum at a high mole fraction of the shortest-chain soap. The minimum indicates that the solid phase is a nonideal mixture of soaps. A one-parameter model for the solid−liquid equilibrium of the soaps at the Krafft temperature describes the data well. Changes in the bilayer spacing of the soap crystals with the solid composition prove that the soaps mix in the solid phase. Finally, solid soaps can contain hydrating water but do not form stoichiometric hydrates.

Acknowledgment. G. C. Merkel is acknowledged for some of the phase behavior and cmc experiments. We benefited from discussions with L. P. Burleva and P. D. T. Huibers. We thank T. P. Labuza for allowing us to use the Karl Fischer instrument and D. Thomas for using the fluorescence spectrometer. This work was supported by Imation Corp. and by the Center for Interfacial Engineering at the University of Minnesota.

LA000467N